Structure and Properties of $HFe_3(CO)_9BH_3R$ and the Conjugate Bases $[HFe_3(CO)_9BH_2R]^-$ (R = H and CH_3). Inorganometallic Analogues of Hydrocarbyltriiron Clusters

Jose Vites,[†] Catherine E. Housecroft,[†] Charles Eigenbrot,[†] Margaret L. Buhl,[‡] Gary J. Long,[‡] and Thomas P. Fehlner*[†]

Contribution from the Department of Chemistry, University of Notre Dame, Notre Dame, Indiana 46556, and the Department of Chemistry, University of Missouri-Rolla, Rolla, Missouri 65401. *Received October 30, 1985*

Abstract: The ferraboranes $(\mu\text{-H})Fe_3(CO)_9BH_3R$ and the conjugate bases $[(\mu\text{-H})Fe_3(CO)_9BH_2R]^-$, R = H and CH_3, have been prepared and characterized. Crystals of $HFe_3(CO)_9BH_4$ form in the space group $P\bar{1}$ with unit cell parameters a = 8.823 (5) Å, b = 11.523 (5) Å, c = 7.850 (4) Å, α = 98.89 (4)°, β = 109.82 (4)°, γ = 87.92 (4)°, V = 741.7 Å^3, and Z = 2. The structure was solved by direct methods and refined to R = 0.061 and R_w = 0.079 for 2157 independent $[F_o \geq 3\sigma(F_o)]$ reflections. The infrared spectra and ^{11}B NMR and dynamic ^1H NMR spectra have been measured for all compounds. Mass spectra and UV-vis spectra are reported for the neutral compounds while the Mössbauer spectrum is reported for one anion (R = H). The neutral compounds can be considered as formal $[\mu_3\text{-}BH_3R]$ triiron clusters. Both the neutral and anionic ferraboranes are isoelectronic with the hydrocarbyliron clusters $(\mu\text{-H})_3Fe_3(CO)_9(\mu_3\text{-CR})$, R = H and CH_3, and the ferraborane anions are isoprotonic with the hydrocarbyls. As such the ferraboranes are inorganometallic analogues of the organometallic clusters. Among other things, a comparison of these clusters yields insight into the factors important in determining stable hydrogen positions on these tetranuclear systems.

Ferraboranes, compounds formally composed of iron- and boron-containing fragments, can be usefully considered as either metal-ligand complexes or heteroatom metal clusters.[1] Viewed as metal-ligand complexes, these compounds are of significant theoretical interest because many are isoelectronic with classic organometallic prototypes. For example, in pointing out some of the similarities and differences between $B_nH_{m+x}^{(n-x)-}$ and C_nH_m as metal ligands,[2] we have emphasized the way the bridging hydrogens in the former compensate for the lack of low-lying π^* orbitals by an orientation (rehybridization) of the principal donor orbital toward the metal atom.[3] We have called such metallaboranes inorganometallic compounds to emphasize their relationship with organometallic compounds.[4]

Here we present the full characterization[5] of two related ferraboranes and their anionic conjugate Brønsted bases. The neutral compounds are isoelectronic with the hydrocarbyls $(\mu\text{-H})_3Fe_3(CO)_9(\mu_3\text{-CR})$, R = H (I) and CH_3 (II) which we have discussed previously.[6,7] In this earlier work, our attention was focused on

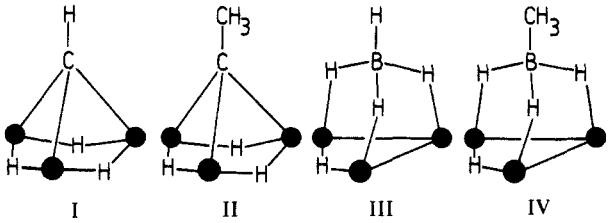

the perturbation of molecular geometry and electronic structure caused by the metal-metal bridging hydrogens while here we present information on the structural role of metal-boron bridging hydrogens.

As is demonstrated below, the boron analogues of the hydrocarbyls, $(\mu\text{-H})Fe_3(CO)_9BH_3R$, R = H (III) and CH_3 (IV), have strikingly different endo-hydrogen locations. Taking the Fe_3X, X = C or B, cluster core as a point of reference, we observe the interesting situation whereby in going from I, II to III, IV the hydrogens move from the triangular metal base to the apical atom—a process akin to reduction of the main group atom. Hence, the factors governing hydrogen positions in these systems should be important in understanding reduction of a main group fragment coordinated to a trimetal site. Here we explore the features of the geometrical and electronic structures of III and IV and the conjugate anions as revealed by structural and spectroscopic experiments. These are contrasted with similar information from the isoelectronic carbon derivatives I and II.

Structure of the Neutral Compounds

The solid-state structure of III consists of discrete molecular units at general positions in the unit cell. The closest intermolecular contact is 3.07 (1) Å between oxygen atoms, and the packing diagram is given in the supplementary material. The molecular structure itself is presented in the ORTEP drawing in Figure 1 where the atoms are represented at 50% thermal elipsoids. The hydrogens were not directly located, and the hydrogen positions shown are derived indirectly as presented below. The molecule III consists of a triangular array of $Fe(CO)_3$ fragments capped by a boron atom. As such, the cluster core is a member of the well-known family of μ_3-capped trimetal clusters[8] such as II. Bond distances and angles are listed in Table I. One of the Fe-Fe bonds is significantly longer than the other two [2.673 (2) vs. 2.603 (2) and 2.592 (2) Å]. The Fe-C-O fragments are unexceptional, but the Fe-Fe-C angles are not all equal and in fact exhibit a pattern correlating with the observed long Fe1-Fe3 bond.[9,10] This is most evident when viewed down the C_3 axis of the Fe_3 triangle as shown in Figure 2. Here the observed CO positions are contrasted with those expected if the CO's were distributed symmetrically about the metal skeleton. Both the metal-metal distances and the orientation of the CO's suggest

[†] University of Notre Dame.
[‡] University of Missouri—Rolla.

(1) Housecroft, C. E.; Fehlner, T. P. *Adv. Organometal. Chem.* **1982**, *21*, 57.
(2) DeKock, R. L.; Deshmukh, P.; Fehlner, T. P.; Housecroft, C. E.; Plotkin, J. S.; Shore, S. G. *J. Am. Chem. Soc.* **1983**, *105*, 815.
(3) Dewar, M. J. S. *Bull. Soc. Chim. Fr.* **1951**, *18*, C71: Chatt, J.; Duncanson, L. A. *J. Chem. Soc., Chem. Commun.* **1953**, 2939.
(4) Fehlner, T. P. 30th IUPAC Meeting, Manchester, Sept 1985.
(5) Vites, J. C.; Eigenbrot, C.; Fehlner, T. P. *J. Am. Chem. Soc.* **1984**, *106*, 4633: Vites, J. C.; Housecroft, C. E.; Jacobsen, G. B.; Fehlner, T. P. *Organometallics* **1984**, *3*, 1591.
(6) Wong, K. S.; Haller, K. J.; Dutta, T. K.; Chipman, D. M.; Fehlner, T. P. *Inorg. Chem.* **1982**, *21*, 3197.
(7) DeKock, R. L.; Wong, K. S.; Fehlner, T. P. *Inorg. Chem.* **1982**, *21*, 3203.
(8) *Transition Metal Clusters*; Johnson, B. F. G., Ed.; Wiley: New York, 1980.
(9) Teller, R. G.; Bau, R. *Struct. Bonding* **1981**, *44*, 1.
(10) Andrews, M. A.; VanBuskirk, G.; Knobler, C. B.; Kaesz, H. D. *J. Am. Chem. Soc.* **1979**, *101*, 7245.

0002-7863/86/1508-3304$01.50/0

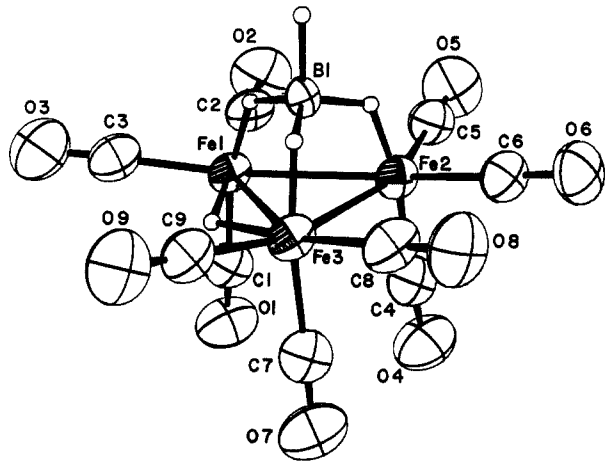

Figure 1. Structure of III. The hydrogen atom locations are based on spectroscopic data.

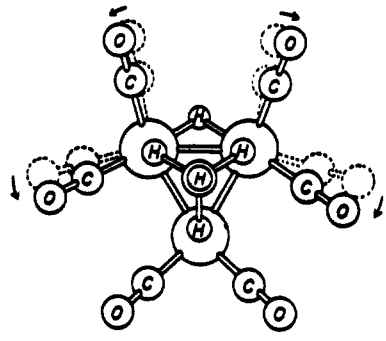

Figure 2. Schematic representation of the displacement of equatorial CO ligands by the metal edge bridging hydrogen.

the presence of a bridging hydrogen between Fe1 and Fe3 placed as shown in Figure 1. The Fe–B bond distances are similar but not identical, those to Fe1 and Fe3 being 0.06 Å longer than that to Fe2. This may also reflect the hydrogen bridging Fe1–Fe3 but, because of the unrefined hydrogen atoms in the vicinity of the boron, no great significance can be placed in these differences. The average Fe–B distance (2.17 Å) is about that expected for an unbridged apical boron–basal iron distance (estimated as 2.15 Å from the sum of covalent radii). For a bidentate borohydride ligand bound to iron, one estimates a range of bridged Fe–B distances of 2.15–2.20 Å from the known structures of other first-row transition-metal complexes.[11] Thus, the Fe–B distances observed in III do not require the presence of hydrogen bridges. Note, however, that the average Fe–B distance in III is greater than that for a "closed" three-center Fe–H–B bond (1.97 Å)[12] and shorter than that in a compound with a formal "open" Fe–H–B bond (2.26 Å).[13]

The solution infrared spectrum in the carbonyl region is shown in Figure 3a. There is no evidence of a bridging carbonyl, but the complexity of the spectrum in the terminal region shows that the symmetry of the $Fe_3(CO)_9$ fragment is lower than C_{3v}. This would be true if there were a bridging hydrogen in the metal base. A weak band at 2335 cm^{-1} indicates the presence of a BH terminal unit. Except for the absence of a BH band, the infrared spectrum of IV is nearly identical with that of III.

The proton NMR at low temperature is shown in Figure 4 and the chemical shifts, relative intensities, and line widths for both III and IV are given in the Experimental Section. ^{11}B–^1H coupling constants could not be measured from the ^1H NMR because of thermal decoupling of proton and boron spins at low temperatures. In terms of the chemical shift, four types of proton environment

(11) Marks, T. J.; Kolb, J. R. *Chem. Rev.* **1977**, *77*, 263.
(12) Fehlner, T. P.; Housecroft, C. E.; Scheidt, W. R.; Wong, K. S. *Organometallics* **1983**, *2*, 825.
(13) Haller, K. J.; Andersen, E. L.; Fehlner, T. P. *Inorg. Chem.* **1981**, *20*, 309.

Table I. Selected Interatomic Distances (Å) and Angles (deg) of III

Distances			
Fe1–Fe2	2.6026 (21)	Fe1–Fe3	2.6732 (22)
Fe2–Fe3	2.5923 (19)	Fe1–C1	1.769 (9)
Fe1–C2	1.811 (9)	Fe1–C3	1.784 (9)
Fe2–C4	1.818 (11)	Fe2—C5	1.803 (9)
Fe2–C6	1.796 (9)	Fe3–C7	1.807 (11)
Fe3–C8	1.798 (9)	Fe3–C9	1.819 (9)
Fe1–B	2.197 (8)	Fe2–B	2.129 (8)
Fe3–B	2.176 (8)	C1–O1	1.146 (10)
C2–O2	1.119 (10)	C3–O3	1.143 (10)
C4–O4	1.129 (11)	C5–O5	1.118 (10)
C6–O6	1.142 (10)	C7–O7	1.128 (11)
C8–O8	1.129 (10)	C9–O9	1.115 (10)
Angles			
Fe1–Fe2–Fe3	61.94 (6)	Fe1–Fe3–Fe2	59.22 (6)
Fe2–Fe1–Fe3	58.84 (5)	Fe1–B–Fe2	73.9 (25)
Fe1–B–Fe3	75.4 (25)	Fe2–B–Fe3	74.0 (25)
C1–Fe1–C2	92.9 (4)	C1–Fe1–C3	96.3 (4)
C2–Fe1–C3	98.2 (4)	C1–Fe1–Fe2	96.1 (3)
C1–Fe1–Fe3	101.3 (3)	C2–Fe1–Fe2	90.7 (3)
C2–Fe1–Fe3	147.3 (3)	C3–Fe1–Fe2	164.3 (3)
C3–Fe1–Fe3	109.2 (3)	Fe1–C1–O1	179.1 (8)
Fe1–C2–O2	179.4 (9)	Fe1–C3–O3	179.4 (9)
C4–Fe2–C5	94.3 (4)	C4–Fe2–C6	94.9 (4)
F5–Fe2–C6	95.8 (4)	C4–Fe2–Fe1	96.3 (3)
C4–Fe2–Fe3	95.6 (3)	C5–Fe2–Fe1	101.8 (3)
C5–Fe2–Fe3	161.8 (3)	C6–Fe2–Fe1	158.3 (3)
C6–Fe2–Fe3	98.6 (3)	Fe2–C4–O4	177.9 (9)
Fe2–C5–O5	177.1 (9)	Fe2–C6–O6	176.6 (9)
C7–Fe3–C8	92.5 (4)	C7–Fe3–C9	97.1 (4)
C8–Fe3–C9	97.0 (4)	C7–Fe3–Fe1	99.7 (3)
C7–Fe3–Fe2	94.5 (3)	C8–Fe3–Fe1	149.7 (3)
C8–Fe3–Fe2	92.5 (3)	C9–Fe3–Fe1	108.7 (2)
C9–Fe3–Fe2	164.7 (3)	Fe3–C7–O7	179.4 (8)
Fe3–C8–O8	178.8 (8)	Fe3–C9–O9	179.5 (8)

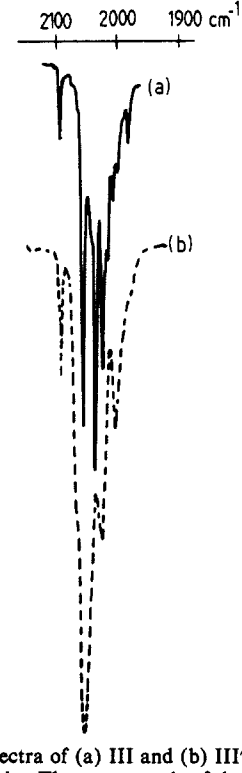

Figure 3. Infrared spectra of (a) III and (b) III′ (PPN salt) in hexane and toluene, respectively. The energy scale of the latter has been shifted 50 cm^{-1} to higher energy.

are observed: one H corresponding to Fe–H–Fe, two H's corresponding to one type of Fe–H–B, one H corresponding to another type of Fe–H–B, and one H corresponding to a terminal BH. The first proves the existence of a metal bridging hydrogen suggested by the solid-state structure and the infrared. The second and third demonstrate that the molecule has a plane of symmetry and that

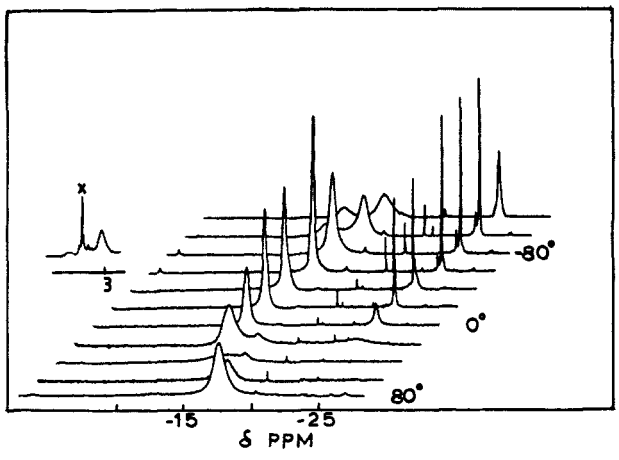

Figure 4. Variable-temperature 300-MHz ^1H NMR spectra of III in $C_6D_5CD_3$. Nominal temperatures decrease in 20 °C steps. The resonance at δ 3.2 (shown in the −80 °C spectrum) sharpens on cooling due to thermal decoupling. The signals at δ 4.1, −17, −20, and −24 are due to known impurities.

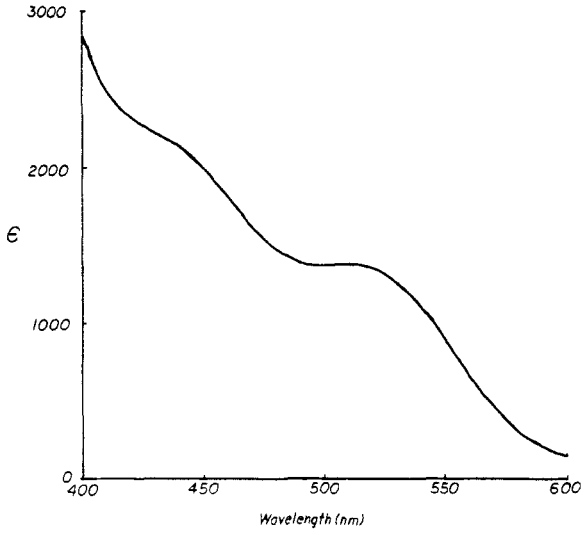

Figure 5. UV–vis spectrum of III in hexane. The units of the extinction coefficient are M^{-1} cm^{-1}.

the Fe–B skeletal edges are hydrogen bridged. The last shows the presence of a terminal hydrogen on boron as suggested by the infrared. Hence, the structure shown in Figure 1 is fully confirmed.

Figure 4 demonstrates that as the temperature is raised, some of the hydrogens of III begin to exchange. At about −50 °C the Fe–H–B protons become equivalent while at 80 °C the Fe–H–B and Fe–H–Fe protons exchange rapidly on the NMR time scale. Up to this temperature, there is no evidence for the participation of the terminal proton in the exchange process. The same qualitative dynamic NMR behavior illustrated in Figure 4 is observed for the *B*-methyl derivative IV, thereby confirming the nonparticipation of the terminal H of III. However, for IV the coalescence of the Fe–H–B and Fe–H–Fe protons is observed about 60° lower than for III, thereby demonstrating a small (about 3 kcal/mol) substituent effect on the barrier for the fluxional process. Because of the lower barrier in IV, the two types of Fe–H–B protons are not frozen out at −90 °C.

The ^{11}B NMR chemical shifts and coupling constants for III and IV are given in the Experimental Section. Substitution of a CH_3 group for a terminal H introduces a downfield shift, but otherwise the parameters are similar. Note that the chemical shifts are at the low edge of the range expected for tetracoordinate boron.[14]

(14) Kidd, R. G. In *NMR of Newly Accessible Nuclei*; Laszlo, P., Ed.; Academic: New York, 1983; Vol. 2, p 50.

Table II. Mössbauer Effect Spectral Parameters[a] for III′

assignment	δ	ΔE_Q	Γ	% area	χ^2
Fe2	−0.042	1.10	0.34	30.4[b]	0.78
Fe1, Fe3	0.009	0.45	0.47	60.8[b]	
impurity	1.41	2.28	0.61	8.8	

[a] All data obtained at 78 K and given in mm/s relative to natural abundance room-temperature α-iron foil. [b] Values constrained to the ratio of 1 to 2.

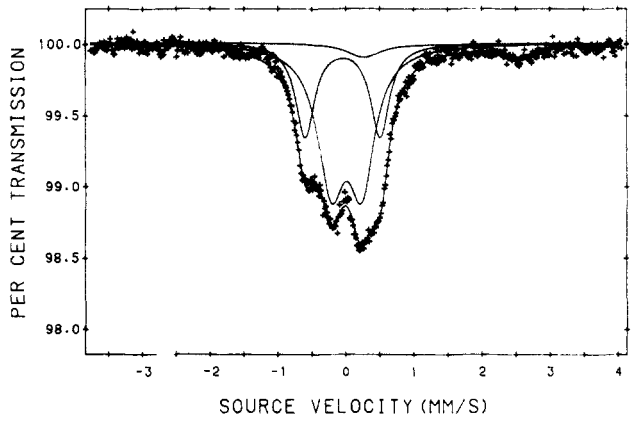

Figure 6. Mössbauer spectrum of III′ obtained at 78 K.

The UV–visible spectrum of IV is shown in Figure 5. The extinction coefficient in the visible spectrum is similar to that observed for other ferraboranes,[15] but the interesting point is that two prominent absorptions are observed in this region. The one with a maximum at 511 nm is similar to the maximum observed for $Co_3(CO)_9CR$ (520 nm) while the maximum at 433 nm is the same as the maximum observed for II. It is tempting to associate the former with the presence of metal–metal bonds and the latter with hydrogen-bridged metal bonds, thus viewing IV as a hybrid of II and $Co_3(CO)_9CR$.

Structure of the Anions

Both III and IV are acids and are readily deprotonated in methanol. In contrast to II which spontaneously loses H_2 upon deprotonation,[16] IV cleanly deprotonates at 25 °C to form a stable anion.

Crystals of both III′ and IV′ have been obtained, but none were of sufficiently good quality for a complete X-ray diffraction study. However, density measurements and unit cell parameters demonstrate that the anions are derived by simple proton loss from III and IV; i.e., there were no gross changes in cluster composition on deprotonation. In addition, refinement of the $As(C_6H_5)_4^+$ salt of III proceeded sufficiently far to show that the basic boron-capped trimetal structure shown in Figure 1 for the neutral is retained in the anion.

The retention of the integrity of the triiron fragment of III including the metal-bridging hydrogen on deprotonation is confirmed by the carbonyl region of the infrared spectrum. This is shown in Figure 3 where it is compared to that of the neutral compound. Although the bands are broader and shifted about 50 cm^{-1} to lower energy due to anionic character, the spectra are similar. Clearly, the symmetry of the Fe_3 fragment is lower than C_{3v}, which is concomitant with the retention of an Fe–H–Fe proton on deprotonation of III.

A confirmation of the solid-state structure of the triiron fragment in III′ comes from its Mössbauer spectrum illustrated in Figure 6 with the spectral parameters shown in Table II. The spectrum shows about 9% of a high-spin iron(II) impurity which does not interfere with the analysis of the spectrum derived from the cluster. The least-squares fit shown in Figure 6 reveals two

(15) Andersen, E. L.; DeKock, R. L.; Fehlner, T. P. *Inorg. Chem.* **1981**, *20*, 3291.

(16) Dutta, T. K.; Vites, J. C.; Fehlner, T. P. *Organometallics* **1986**, *5*, 385.

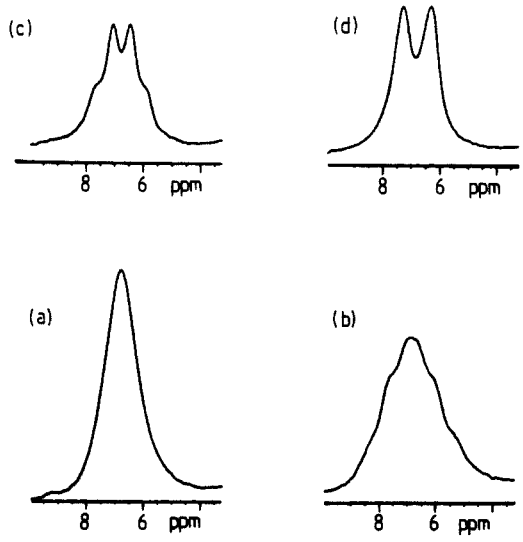

Figure 7. Selective decoupling of the 96.3-MHz ^{11}B NMR spectrum of III′ (PPN) in acetone at 20 °C. (a) $^{11}B\{^1H\}$, (b) fully coupled, (c) $^{11}B\{^1H = 3.8\}$ (J_{BH} = 58 Hz), (d) $^{11}B\{^1H = -13.1\}$ (J_{BH} = 96 Hz).

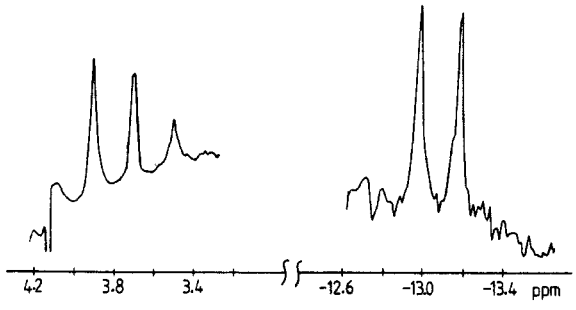

Figure 8. ^1H NMR (100 MHz) $\{^{11}B\}$ (J_{HH} = 20 Hz).

partially resolved quadrupole doublets with the area constrained ratio of 2 to 1. If this constraint is relaxed, virtually the same fit is obtained but with an area ratio of 1.94 to 1. The presence of the two doublets in this ratio confirms the presence of two inequivalent iron sites and is consistent with the presence of a bridging hydrogen in the trimetal base of III′. The observed higher relative isomer shift for the two equivalent iron sites, which is indicative of a lower s-electron density than at the other site, indicates the importance of the valence s-electron delocalization from the iron onto the bridging hydrogen. A similar relative increase in iron isomer shift values of iron sites bridged by hydrogens has been recently reported[17] in two "butterfly" structures.

The ^{11}B chemical shifts and B–H coupling constants for III′ and IV′ are given in the Experimental Section. There is a small downfield shift on deprotonation and a small increase in the coupling constants; however, the multiplicity of the splitting evident in the selective $\{^1H\}$ experiments (Figure 7) shows that the boron is coupled to three equivalent Fe–H–B protons at 25 °C. As the data above suggest the presence of a Fe–H–Fe proton, these observations can only be simultaneously true if the anion is fluxional; i.e., two Fe–H–B protons are scrambling with the metal-bridging proton. Because coupling is observed in the fast-exchange limit, the process must be intramolecular.

The ^1H NMR data on III′ and IV′ are given in the Experimental Section, and the $\{^{11}B\}$ resonances of III′ are shown in Figure 8. The data show the presence of one B–H terminal proton and, down to −90 °C, three magnetically equivalent skeletal protons. Indeed, as shown in Figure 8, the geminal coupling of the two types of protons confirms the multiplicity. Again, to accommodate the Mössbauer and IR structural data based on shorter time scales than the NMR data, we must postulate a process that makes the Fe–H–Fe and Fe–H–B protons equivalent. Although we cannot eliminate a structure with two metal hydrides and one metal–boron bridge, the observed ^{11}B chemical shift suggests only one of the former. Hence we postulate the static structures shown below for III′ and IV′. The net result of deprotonation, then, is the loss of a Fe–H–B proton.

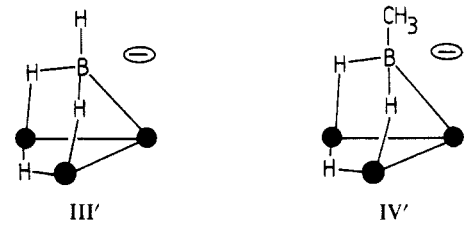

III′ IV′

Discussion

As was pointed out in the Introduction, III and IV are isoelectronic with I and II. Hence an important point to address is the difference between the structural and spectroscopic properties of these compounds which differ only in the spatial locations of protons. The most striking difference in geometry is the orientation of the CO's relative to the iron triangle. Recall that in discussing the structure of II relative to that of $Co_3(CO)_9CR$, the "tilt"[6] of the octahedral $M(CO)_3$ fragment was shown to be one indicator of the effect of the MHM hydrogens on the apical basal bonding interaction. The average dihedral angle between the M_3 triangle and the plane defined by $(CO)_e$–M–$(CO)_e$, where e refers to the equatorial CO's, for $Co_3(CO)_9CR$, II, and III is 29°, 42°, and 16°, respectively. Hence, the equatorial CO's in III lie much more nearly in the metal plane than do those of II or even $Co_3(CO)_9CR$. The schematic structural comparison for I–IV emphasizes this point. In III the axial CO of each $Fe(CO)_3$ fragment is nearly perpendicular to the plane of the three metal atoms while in II they are substantially tilted away from the vertical. This geometric feature is clearly related to the different placement of the hydrogens in I and III and suggests that a given CO orientation results from the different hydrogen locations rather than vice versa.

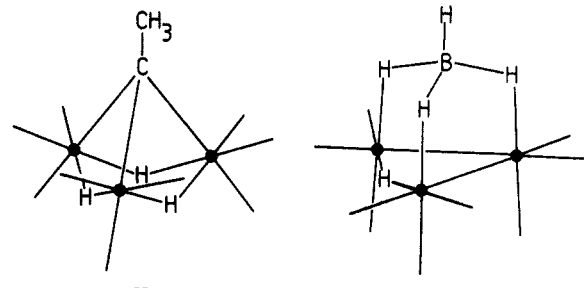

II III

Further information on the nature of the bonding of the apical atoms of I and III to the triiron framework is revealed by comparison of the ^{11}B and ^{13}C chemical shifts. This is facilitated by the existence of a correlation between ^{11}B chemical shifts of boranes and ^{13}C chemical shifts of closely related compounds.[18] Using this correlation and the observed ^{13}C shifts for I[19] and II,[20] one calculates δ 48 and δ 60 for III and IV compared to the observed values of 2 and 22. The observed downfield shift caused by CH_3 substitution is reproduced in the estimated chemical shifts. However, values of the calculated shifts for III and IV are at substantially lower field than the observed values. Although no correlation is perfect, the observed ^{13}C shift for the anion I′,[19] which possesses a C–H–Fe interaction, yields a calculated δ 9 for

(17) Benson, C. G.; Long, G. J.; Bradley, J. S.; Kolis, J. W.; Shriver, D. F. *J. Am. Chem. Soc.*, in press.

(18) Spielvogel, B. F.; Nutt, W. R.; Izydore, R. A. *J. Am. Chem. Soc.* **1975**, *97*, 1609. Nöth, H.; Wrackmeyer, B. *Chem. Ber.* **1974**, *107*, 3089. Williams, R. E.; Field, L. D. *Boron Chemistry-4*; Parry, R. W., Kodama, G., Eds.; Pergamon: New York, 1980; p 131.

(19) Vites, J. C.; Jacobsen, G. J.; Dutta, T. K.; Fehlner, T. P. *J. Am. Chem. Soc.* **1985**, *107*, 5563.

(20) Kolis, J. W.; Holt, E. M.; Shriver, D. F. *J. Am. Chem. Soc.* **1983**, *105*, 7307.

III′ compared to an observed value of δ 6. This suggests that

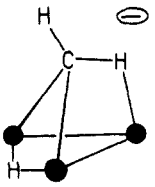

I′

the former discrepancy between measured and calculated shifts for III and IV reflects a real difference in the environments of the carbon vs. boron apices. We attribute this to the presence or absence of hydrogens bridging the Fe–B or Fe–C edges.

In contrast to chemical shifts, coupling constants provide information more directly related to the chemical bonding of the coupled nuclei. A comparison of the ^{13}C–^{1}H and ^{11}B–^{1}H coupling constants in I and III and the respective anions is facilitated by a straightforward relationship between B–H and C–H coupling constants.[21] The measured values for I and I′ have been reported[19] while those for III and III′ are given in the Experimental Section. Thus, the values for B–H(terminal) coupling for Fe_3B clusters with zero, one, two, and three Fe–H–B interactions are [119], [105], 96, and 75 Hz where the values in brackets are calculated from the relationship $J_{BH} = 0.7J_{CH}$. These coupling constants show that as hydrogens are moved from the iron base to Fe–X bridging positions in going from I to III, there is a smooth decrease in the B–H coupling constant (Figure 9). As coupling constants reflect the product of the boron and hydrogen valence orbital s characters, this suggests a similar change in the hybridization of the capping atom. Hence, the coupling constants confirm, as well as define more precisely, the change in capping atom–trimetal base bonding caused by the addition of hydrogens bridging the FeX edges.

Another question raised by the isolation and characterization of III is the proper description of the structure. Is it the first example of a μ_3-BH_4^- ligand bound to a trimetal framework, or is it a hydrogenated tetranuclear triiron boron cluster? The comparison with the carbon analogues (see above) suggests that the description of III as a four atom Fe_3B cluster with four endo hydrogens is very appropriate. Still the geometrical information and the NMR parameters, presented above, show that III can be adequately described as a BH_4^- ligand triply bridging a 42-electron $HFe_3(CO)_9^+$ fragment. Each of the three B–H bonds of the borohydride ligand that forms a bridging interaction donates two electrons, yielding a 48-electron trimetal system.[22] Clearly, the answer to the question posed must be sought in information that is intrinsically very sensitive to structural nuances.

Fluxional processes observed by NMR spectroscopy have low barriers and therefore are sensitive to small perturbations in structure and bonding.[23] The fluxional behavior of III and III′ demonstrates that skeletal B–H bond breakage occurs in preference to Fe–H bond rupture. However, it is commonly observed in borohydride metal complexes that all bridge and terminal hydrogens rapidly scramble on the NMR time scale (Fe–H bond breakage in preference to B–H).[11] In fact there are only a few examples in which this dynamic process has been frozen out.[11,24] In III the coordination of the BH_4 moiety has gone beyond that in a normal mononuclear complex.[25] The bridging hydrogens, which are derived from terminal hydrogens in the free BH_4^- ligand, are no longer as closely associated with the boron atom as they are in typical mononuclear complexes. That is, the fact that the

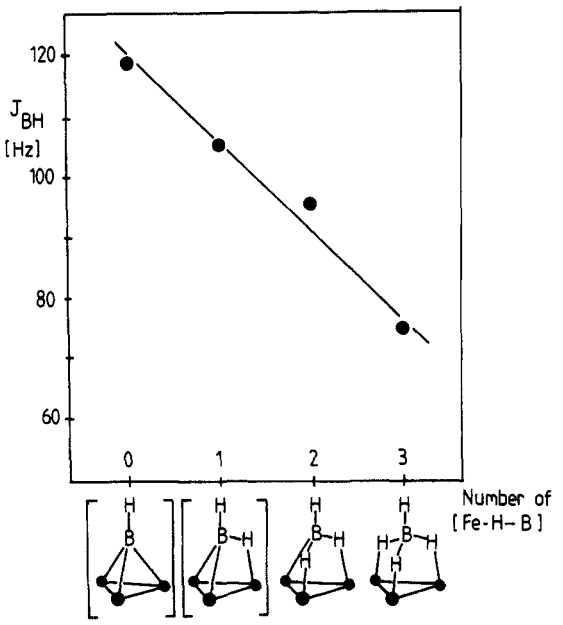

Figure 9. Plot of J_{BH} (terminal) vs. number of Fe–H–B interactions.

Fe–H–B hydrogens do not exchange with the terminal B–H whereas they do exchange with the Fe–H–Fe hydrogen may be viewed as evidence that the Fe–H–B and Fe–H–Fe hydrogens are more alike than the Fe–H–B and B–H hydrogens. As the energy window separating static and fully exchanging systems on the NMR time scale is small, this difference is a subtle one which might not be reflected in the geometric parameters.

Although III and IV are fluxional at room temperature, the hydrogen-scrambling process can be frozen out. On the other hand, III′ and IV′ are fluxional even at low temperature. Likewise, the hydrogens of I, which are not fluxional, undergo rapid exchange on the NMR time scale after deprotonation. Thus, for both sets of compounds, deprotonation results in a rate enhancement of hydrogen-exchange processes. A similar observation for carbonyl-exchange processes has been reported for larger cluster systems.[26]

A final comparison concerns the behavior of the two sets of compounds on deprotonation. Deprotonation of III and IV leads to stable anions in which a Fe–H–B proton has been removed. Deprotonation of I[19] leads to rearrangement with the loss of a Fe–H–Fe proton while deprotonation of II leads to the production of an unstable anion that immediately loses H_2.[16] Hydrogen loss for IV can be induced by heating, but the barrier for H_2 loss is much higher for the ferraborane vs. the hydrocarbyl complex. As the mechanism suggested for the latter involves the formation of terminal hydrides from bridging hydrides,[16] the difference may reflect the strength of the Fe–H–B interaction. So even in terms of simple proton loss, the compounds are significantly different.

Conclusions

The intercomparison of the structures and spectroscopic properties of I–IV and their conjugate anions has delineated some of the consequences of the various ways of distributing three through five hydrogens on the edges of a capped triiron cluster. As I is a viable model for dissociated CH_4 on a trimetal surface site[27] whereas III is an equally viable model for chemisorbed CH_4 on a trimetal surface site, this series of compounds constitutes a model system for studying the factors that control the formation and cleavage of C–H bonds on a metal surface. As the location

(21) Onak, T.; Leach, J. B.; Anderson, S.; Frisch, M. J. *J. Magn. Reson.* **1976**, *23*, 237.
(22) Lauher, J. W. *J. Am. Chem. Soc.* **1978**, *100*, 5305.
(23) Band, E.; Muetterties, E. L. *Chem. Rev.* **1978**, *78*, 639.
(24) Empsall, H. D.; Mentzer, E.; Shaw, B. L. *J. Chem. Soc., Chem. Commun.* **1975**, 861.
(25) There is one example of a mononuclear complex in which the M–H–B protons exchange more rapidly with M–H than with B–H protons. Frost, P. W.; Howard, J. A. K.; Spencer, J. L. *J. Chem. Soc., Chem. Commun.* **1984**, 1362.
(26) Martinengo, S.; Heaton, B. T.; Goodfellow, R. J.; Chini, P. *J. Chem. Soc., Chem. Commun.* **1977**, 39.
(27) Note that the osmium derivative of I has been reported to generate CH_4 when treated with Lewis bases. A structure similar to III is a very reasonable intermediate or transition state in the process. Calvert, R. B. Ph.D. Thesis, University of Illinois, Urbana, 1978. As referenced by: Muetterties, E. L. *Chem. Rev.* **1982**, *11*, 283.

Table III. Summary of Crystal Data and Intensity Collection Parameters for $HFe_3(CO)_9BH_4$

formula	$Fe_3O_9C_9BH_5$
fw, amu	435.49
cryst dimensions, mm	0.30 × 0.30 × 0.10
radiation	graphite monochromated Mo Kα, λ = 0.1073 Å
temp, °C	18 ± 1
space group	$P\bar{1}$
a, Å	8.823 (5)
b, Å	11.523 (5)
c, Å	7.850 (4)
α, deg	98.89 (4)
β, deg	109.82 (4)
γ, deg	87.92 (4)
V, Å^3	741.7
Z	2
density (calcd), g/cm^3	1.950
density (obsd), g/cm^3	1.875
diffractometer	Syntex $P\bar{1}$
scan type	$\theta/2\theta$
scan range	0.70° below $K\alpha_1$ to 0.70° above $K\alpha_2$
2θ limits, deg	3.5–54.9
background	0.5 times scan time at extreme of scan
reflections included	2157 with $F_o > 3.0\sigma(F_o)$
R	0.061
R_w	0.079
goodness of fit	1.88
data/parameter	10.84

of a proton in a molecule is one of the least complex (but not simple) problems to treat theoretically, these compounds also present a challenge to the theorist.

Experimental Section

General. All reactions and manipulations were carried out under inert atmospheres or in a vacuum line with standard techniques.[28] Solvents were dried (toluene over anhydrous $MgSO_4$, THF over KOH pellets, hexane over molecular sieve), degassed, and distilled before use; methanol and dichloromethane were dried over molecular sieve and degassed before use. The following were used as received: $Na_2[Fe(CO)_4]$ (Alfa); $[Ph_4As]Cl$ and [PPN]Cl [bis(triphenylphosphine)(iminium) chloride] (Aldrich); CF_3COOH (Aldrich). H_3PO_4 (Fisher, 85%) was degassed before use. $CH_3C(O)Cl$ (Fisher) and NEt_3 (Eastman) were distilled prior to use. BH_3·THF (1 M, Aldrich) was titrated before use.[29] Chromatography was performed on 60–200-mesh silica gel (Baker). ^{11}B and ^1H FT NMR spectra were obtained on a Nicolet 300-MHz spectrometer, the $^{11}B\{^1H\}$ spectra were obtained on a Varian XL-100 spectrometer, infrared spectra were recorded on a Perkin-Elmer 983 spectrometer, mass spectra were run on a AEI-MS 9 spectrometer, and UV–vis spectra were obtained on a Varian DMS-100 spectrometer. ^{11}B shifts are reported with respect to BF_3·OEt_3 (δ 0) and ^1H shifts with respect to TMS (δ 0).

The Mössbauer effect spectra were obtained at 78 K on a conventional Ranger Scientific constant acceleration spectrometer which utilized a room-temperature rhodium-matrix cobalt-57 source and was calibrated at room temperature with natural abundance α-iron foil. The spectra were fit to Lorentzian line shapes by using standard least-squares computer minimization techniques.

Preparation of III. Commercial BH_3·THF (4 mmol) was added to $[(CO)_4FeC(O)CH_3]Na$ in 20 mL of THF at 25 °C with stirring. CO and H_2 were evolved, and the solution turned a deep brown. After the solution was heated at 65 °C for 30 min, the solvent was removed and the residue acidified with H_3PO_4 (85%) in the presence of 3 × 10 mL aliquots of hexane. Chromatography with hexane yielded several bands. The second band (orange) was collected. Recrystallization from hexane at −10 °C yielded red–orange needles in about 5% yield based on iron: MS, *m/e* P^+ 436 (−9CO), $^{56}Fe_3{}^{11}B^1H_5^+$ measd 183.855, calcd 183.853; IR ν_{CO} (hexane, cm^{-1}) 2096 m, 2061 s, 2042 s, 2030 s, 2021 s, 2013 s, 1998 m; ^1H NMR ($C_6H_5CD_3$, −90 °C) δ 3.2 (br s, 1 H), −12.8 (br s, 1 H), −15.8 (br s, 2 H), −24.4 (s, 1 H); ^{11}B NMR (C_6D_6, 20 °C) δ 1.8 (br m, *J* = 230 Hz, fwhm), $\{^1H\}$ (br s, *J* = 150 Hz, fwhm).

Crystal Structure of III. Preliminary examination of a red–orange crystal of III revealed a two-molecule triclinic cell. Indexing of 15 automatically centered reflections between 25° and 30° in 2θ yielded the cell parameters specified in Table III. A total of 3982 reflections were collected, of which 2157 were used in the final refinement.[30] The intensities of 4 reflections measured every 50 reflections remained constant within experimental error. The structure was solved by direct methods.[31] The isotropic model converged to $R = 0.14$ and $R_w = 0.16$.[32] An empirical absorption correction was applied. The correction factor ranged from 0.65 to 1.27 on F_o. The merging *R* for 308 averaged reflections was 5.4% based on I. The anisotropic model converged to $R = 0.061$ and $R_w = 0.079$. Hydrogen atoms were not found and were not included in the model. The largest peak in the final difference Fourier map was 1.2 e$^-$/Å^3, 1 Å from both C9 and Fe3. The residuals showed no anomalies. Final positional parameters are given in Table IV while thermal parameters appear in the supplementary material.

Table IV. Fractional Coordinates[a]

atom	*x*	*y*	*z*
Fe1	0.37242 (12)	0.22984 (10)	0.37853 (15)
Fe2	0.26919 (13)	0.29619 (10)	0.05694 (16)
Fe3	0.06384 (12)	0.19914 (10)	0.16439 (15)
O1	0.3637 (9)	0.4610 (6)	0.5866 (11)
O2	0.7076 (7)	0.2611 (7)	0.4029 (11)
O3	0.4334 (9)	0.0997 (7)	0.6865 (11)
O4	0.2001 (10)	0.5409 (6)	0.1792 (11)
O5	0.5687 (8)	0.3550 (8)	0.0062 (11)
O6	0.0736 (8)	0.2966 (7)	−0.3293 (9)
O7	−0.0651 (8)	0.4228 (6)	0.2858 (10)
O8	−0.1824 (7)	0.1728 (7)	−0.2003 (9)
O9	−0.0951 (8)	0.0479 (6)	0.3235 (9)
C1	0.3682 (10)	0.3704 (8)	0.5046 (12)
C2	0.5793 (10)	0.2494 (8)	0.3928 (12)
C3	0.4096 (10)	0.1500 (8)	0.5657 (13)
C4	0.2260 (11)	0.4465 (9)	0.1350 (12)
C5	0.4549 (11)	0.3347 (8)	0.0293 (13)
C6	0.1456 (10)	0.2974 (8)	−0.1777 (12)
C7	−0.0160 (10)	0.3369 (9)	0.2382 (12)
C8	−0.0869 (10)	0.1840 (7)	−0.0599 (13)
C9	−0.0353 (9)	0.1056 (8)	0.2629 (11)
B(1)	0.2735 (9)	0.1201 (7)	0.1095 (10)

[a] The estimated standard deviations of the least significant digits are given in parentheses.

Preparation of III′. III′ can be prepared by the deprotonation of III in the same manner as IV′ (see below). However, it is more convenient to prepare the PPN salt directly as follows. Over a period of a minute, BH_3·THF (6 mmol) was added to a suspension of $[(CO)_4FeC(O)CH_3]PPN$[33] (1.498 g, 2 mmol) in 20 mL of hexane at 25 °C. The mixture was held at 60 °C for 2 h with stirring under a nitrogen purge after which it was cooled to room temperature. Acidification of the reaction mixture using 40% aqueous H_3PO_4 (20 mL) for 2 h lead to the formation of a dark yellow–brown hexane solution and a red–brown solid residue. After removal of the hexane solution, the anionic products from the residue were extracted with toluene (20–40 mL). After removing the solvent under vacuum, the product mixture was chromatographed using CH_2Cl_2:toluene (4:1) eluant, and the red–orange III′ was separated in 8–10% yield as the second fraction: IR ν_{CO} (toluene, cm^{-1}) 2045 m, 1990 sh, 1983 vs, 1954 s, 1933 m; ^1H NMR ($CD_3C(O)CD_3$, −90 °C) δ 7.73–7.56 (m, 30 H) PPN^+, 3.8 (br, 1 H), −13.1 (br, 3 H), $\{^{11}B\}$ 3.8 (q, J_{HH} = 20 Hz), −13.1 (d, J_{HH} = 20 Hz); ^{11}B NMR ($CD_3C(O)CD_3$, 20 °C) δ 6.2 (br dq), $\{^1H\}$ (J_{BH} = 96 Hz (term), J_{BH} = 58 Hz (bridge)).

Crystals of the $[Ph_4As^+]$ salt form in the monoclinic *Ia* space group with the cell parameters *a* = 14.278 (11) Å, *b* = 17.189 (6) Å, *c* = 14.446

(28) Shriver, D. F. *Manipulation of Air Sensitive Compounds*; McGraw-Hill: New York, 1975; p 241.

(29) Brown, H. C. *Organic Synthesis via Boranes*; Wiley: New York, 1975; p 241.

(30) The net intensities were reduced to relative squared amplitudes, $|F_o|^2$, by application of the Lorentz and polarization factor. Standard deviations were calculated from $\sigma^2(F_o) = [Ct + k^2B + p^2(Ct - kB)^2]/[4|F_o|^2(Lp)^2]$ where Ct is the count of the scan, *k* is the ratio of scan time to background counting time, *B* is the total background, and $p = 0.04$.

(31) Programs used in this study included the Enraf-Nonius SDP package and local modifications of Jacobson's ALLS, Zalkins's FORDAP, and Busing and Levy's ORFFE. Atomic form factors were from: Cromer, D. T.; Waker, J. T. *International Tables for X-ray Crystallography*; Kynock: Birmingham, England, 1974; Vol. IV, Table 2.2B. Real and imaginary corrections for anomalous dispersion in the form factor for Fe atoms were from: Cromer, D. T. *Ibid.* Table 2.3.1.

(32) $R = \sum(|F_o| - |F_c|)/\sum|F_o|$ and $R_w = [\sum w(|F_o| - |F_c|)^2/\sum w(F_o^2)]^{1/2}$.

(33) Alper, H.; Tanaka, M. *J. Am. Chem. Soc.* **1979**, *101*, 4245.

(14) Å, $\beta = 96.16\ (7)°$, $V = 3525$ Å^3, and $Z = 4$. The measured density was 1.585 g/cm^3, yielding a measured formula weight of 841.2. The calculated formula weight of $[Ph_4As^+]$ III′ is 817.3.

Preparation of IV. In a typical reaction, $[Et_3BH]Li$ (6 mmol) was added to $Fe(CO)_5$ (5 mmol) in 20 mL of hexane at 0 °C and stirred for 10 min. Commercial BH_3·THF (10 mmol) was added over a period of several minutes, causing the color of the reaction solution to change from pale yellow to dark brown. After the solution was stirred at 0 °C for 1.5 h, the solvent was removed at room temperature, leaving a brown solid residue. This was acidified with H_3PO_4 (25 mL, 40% aqueous), and the neutral ferraborane and hydrocarbyl products were extracted with hexane (3 × 25 mL), yielding a brown-green solution. Subsequent extractions contained mainly $Fe_3(CO)_{12}$. The orange ferraborane IV was separated from the product mixture as the third fraction by column chromatography (hexane) carried out at −40 °C: MS, m/e P^+ 450 (−9CO), $^{56}Fe_3{}^{12}C_{10}{}^{16}O_9{}^{11}B^1H_7$ measd 449.823, calcd 449.823; IR ν_{CO} (hexane, cm^{-1}) 2095 m, 2064 sh, 2057 vs, 2044 s, 2037 vs, 2025 vs, 2015 s, 2006 m, 1982 m; ^{1}H NMR (CD_2Cl_2, −80 °C) δ 1.03 (s, 3 H), −14.6 (br, 3 H), −24.0 (s, 1 H); ^{11}B NMR (hexane, 20 °C) δ 22.1 (quintet, $J_{BH} = 40$ Hz).[34]

Preparation of IV′. Deprotonation of IV was carried out by stirring a hexane solution (20 mL) of the neutral ferraborane with a solution of Ph_4AsCl (or PPNCl) in methanol. The hexane layer was rapidly decolorized, and the methanol layer became deep red. After the methanol layer was separated, the methanol was removed and the residue extracted with ether. Removal of the ether yielded the final product: IR ν_{CO} (THF, cm^{-1}) 2045 m, 2000 vs, 1978 vs, 1956 vs, 1935 m; ^{1}H NMR ($CD_3C(O)CD_3$, 20 °C) δ 7.87 (m, 20 H), Ph_4As^+ 1.09 (s, 3 H), −12.9 (br, 3 H); ^{11}B NMR ($CD_3C(O)CD_3$, 20 °C) δ 29.3 (br q, $J_{BH} = 53$ Hz).

(34) Significant amounts of the ethyl derivative are formed as well, but little III is observed.

Acknowledgment. The support of the National Science Foundation under Grant CHE 8408251 and the Petroleum Research Fund, administered by the American Chemical Society, is gratefully acknowledged. We thank Reynaldo Barreto for the UV-vis spectrum and Grant B. Jacobsen and Fung-E. Hong for assistance with the preparative work and NMR studies.

Registry No. III, 92055-43-1; III′, 101810-38-2; III$[Ph_4As^+]$, 101810-39-3; IV, 101834-61-1; IV′$[Ph_4As^+]$, 101810-41-7; $[(CO)_4FeC(O)CH_3]Na$, 64867-63-6; $[(CO)_4FeC(O)CH_3]PPN$, 36464-58-1; $Fe(CO)_5$, 13463-40-6; $[Et_3BH]Li$, 22560-16-3; BH_3·THF, 14044-65-6.

Supplementary Material Available: Listing of observed and calculated structure factor amplitudes, thermal parameters, and the packing diagram (10 pages). Ordering information is given on any current masthead page.

Chiral Separation of Heterocyclic Drugs by HPLC: Solute–Stationary Phase Base-Pair Interactions

Binyamin Feibush,*† Alvaro Figueroa, Rosita Charles,‡ Kay D. Onan, Pnina Feibush, and Barry L. Karger*

Contribution from the Barnett Institute and Department of Chemistry, Northeastern University, Boston, Massachusetts 02115. *Received October 28, 1985*

Abstract: Hydrogen bonding between a chromatographic stationary phase and several classes of drug molecules has been explored as a means to effect HPLC chiral separation. *N,N′*-2,6-Pyridinediylbis[alkanamides] have been shown by NMR and X-ray diffraction to be complementary to the drug classes of interest and to form a highly specific triple hydrogen bond complex. A derivative of optically active *N,N′*-2,6-pyridinediylbis[(*S*)-2-phenylbutanamide] was bonded to silica gel and used in an HPLC column to separate racemic mixtures of barbiturates (**1**), glutarimides (**3**), and hydantoins (**4**). Mechanistic models of chiral resolution are suggested for these three classes of drugs. No chiral separation was effected for succinimides (**5**). Methylation of an imido nitrogen of these drugs resulted in disruption of the complementarity; therefore, such *N*-methyl derivatives were unretained by the column. This type of bonded phase would appear to offer high potential for separation of closely related species.

Hydrogen bonds are one of the key factors through which a biological system "recognizes" another system on a molecular level. For example the well-known double helix structure of double-stranded DNA is formed by hydrogen bonding between complementary pairs of purine and pyrimidine bases on the two polynucleotide strands. Pairs of these heterocyclic bases can form a hydrogen bonded complex only if there is an appropriate juxtaposition of acid/base character and if complementary functionalities are coplanar and in the correct orientation.

Broad classes of drugs have structural similarities to the bases found in nucleic acids. For example, as shown in Figure 1, glutarimides, barbiturates, succinimides, and hydantoins have similarities to uracil and thymine. These drugs form associates with adenine similar to those found in the base pairs of adenine–thymine and adenine–uracil.[1] Such associations with adenine and its derivatives have been suggested to be in part the basis of the pharmacological activity of these drugs.[2] In addition, IR studies have shown that barbiturates can displace derivatives of uracil or thymine from associates with 9-ethyladenine; however, no pairing of the barbiturates was detected with the other bases.[1] In similar studies, the glutarimides, hydantoins, and succinimides were demonstrated to complex with adenine and not with the other bases.[3] Recent studies employing IR, near IR, and proton NMR have further explored the displacement of thymine from adenine by barbiturates.[4] Such interactions have been proposed to be important in anaesthesia.[5]

The use of hydrogen bonding associates for achievement of separation in chromatography is well established, in both gas chromatography[6,7] and liquid chromatography.[8,9] Moreover,

† Supelco Inc., Bellefonte, PA.
‡ Department of Organic Chemistry, Weizmann Institute of Science, Rehovot, Israel.

(1) Kyogoku, Y.; Lord, R. C.; Rich, A. *Nature (London)* **1968**, *218*, 69–72.
(2) Bush, M. T. *Physiological Pharmacology*; Academic: New York, 1963; Vol. I, p 185–218.
(3) Yu, N. T.; Kyogoku, Y. *Biochim. Biophys. Acta* **1973**, *331*, 21–26.
(4) Buchet, R.; Sandorfy, C. *J. Phys. Chem.* **1984**, *88*, 3274–3288.
(5) Buchet, R.; Sandorfy, C. *J. Phys. Chem.* **1983**, *87*, 275–280.
(6) Gil-Av, E.; Feibush, B.; Charles, R. *Tetrahedron Lett.* **1966**, 1009–1015.

0002-7863/86/1508-3310$01.50/0